UNIT MEMBRANE PARAMETERS OF ELECTRICALLY SYNCYTIAL TISSUES

DAVID N. LEVIN, *Departments of Medicine and the Pharmacological and Physiological Sciences, University of Chicago, Chicago, Illinois 60637*

ABSTRACT A change in the holding voltage, exposure to channel-blocking agents, and similar interventions will induce changes in the membrane properties of electrically syncytial tissues. The altered membrane characteristics will produce changes in the input resistance (R_{IN}) and the phase angle (ϕ) of the complex admittance of the whole preparation. Exact geometry-independent formulas are derived that give the intervention-induced changes in the membrane capacitance and conductance in terms of the measured changes in R_{IN} and ϕ. The formulas automatically account for the effects of extracellular resistance in tissues such as skeletal muscle fibers, cardiac Purkinje fibers, and small cardiac "aggregates." The size, shape, and resistance of the extracellular space may be arbitrary and need not be measured. The surface (invaginated) membranes, which face the bath (extracellular space), are assumed to be characterized by an RC circuit with specific capacity C_{me} (C_{mi}) and specific conductivity g_{me} (g_{mi}). It is assumed that the intracellular voltage gradient between the electrodes and the membranes is negligible or reliably calculable. The intervention is assumed to leave the geometry and resistivity of the extracellular space unchanged. Under these circumstances the intervention-induced changes in C_{me}, C_{mi}, g_{me}, and g_{mi} are determined exactly in terms of the corresponding changes in R_{IN} and certain frequency domain integrals over ϕ. The technique is illustrated by synthetic data for R_{IN} and ϕ generated by the "disk" model of a skeletal muscle fiber in which C_{me} and C_{mi} depend upon holding voltage. The corresponding voltage dependence of R_{IN} and ϕ is successfully "inverted" to expose the underlying voltage dependence of C_{me} and C_{mi}. These computations suggest that the formulas for C_{me} and C_{mi} will be useful in realistic situations, since they are not too sensitive to experimental error in the data for R_{IN} and ϕ. This method makes it possible to detect voltage-dependent capacity changes due to unit membrane processes (e.g., charge movement) as long as the intrinsic time constant of that process is very small (e.g., $<1/30$ ms). As a second example I consider a disk model that is exposed to increasing concentrations of a channel-blocking agent. The drug dependence of R_{IN} and ϕ is used to calculate the drug dependence of the total membrane conductivity (the sum of g_{me} and g_{mi}, weighted by the areas of surface and invaginated membranes, respectively).

I. INTRODUCTION

Many tissues contain invaginated membranes (e.g., the T system of skeletal muscle fibers) or intercellular spaces (e.g., the extracellular space in cardiac muscle or Purkinje fiber preparations). Therefore, current that flows through the invaginated membrane (facing the extracellular space) encounters significant extracellular resistance on its way to the bath. This means that the electrical properties of the whole tissue are a complicated composite of the unit membrane characteristics and the effects of extracellular resistance. Thus, the electrical measurements on a preparation must be manipulated theoretically to expose the underlying properties of the membranes. Previous attempts to do this have relied upon detailed models of the geometry and resistivity of the extracellular space. In the preceding paper (Levin, 1981)

an exact geometry-independent formula was derived for the magnitude of the external surface membrane capacity (C_{me}) in terms of the input resistance (R_{IN}) and the phase angle (ϕ) of the complex admittance of a preparation. It is not difficult to show that the absolute magnitudes of other membrane parameters (e.g., invaginated membrane capacitance, C_{mi}; surface and invaginated membrane conductance, g_{me} and g_{mi}) cannot be determined by electrical measurements on the whole preparation. In this paper I consider interventions that induce changes in C_{me}, C_{mi}, g_{me} and g_{mi} without changing the geometry or resistivity of the extracellular space. Exact model-independent formulas are derived for deducing the intervention-induced *changes* in these membrane parameters from the corresponding changes in R_{IN} and ϕ.

The possibility of deriving such formulas is suggested by considering what happens to R_{IN} and ϕ when each membrane parameter is varied separately. R_{IN} is expected to increase (decrease) when g_{me} or g_{mi} is decreased (increased). On the other hand, R_{IN} is unaffected by changes in C_{me} or C_{mi}, since the pattern of DC current flow is unchanged. These observations are recorded in the first column of Table I. At very low frequencies (lower than the inverse of 2π times the longest time constant of charging of the invaginated membrane) the preparation will behave like a single uninvaginated cell. The phase angle will be approximated by $\tan^{-1}(2\pi\nu\tau_\phi)$, where ν is the frequency in hertz, and τ_ϕ represents the average of the time constants of the external and invaginated membranes (C_{me}/g_{me} and C_{mi}/g_{mi}) weighted by their relative surface areas. Therefore, as C_{me} or C_{mi} is increased (decreased), we expect ϕ to increase (decrease) at low frequencies. Similarly, a decrease (increase) of g_{me} or g_{mi} will cause an increase (decrease) in the low ν values of ϕ. These effects are illustrated by the synthetic data in Fig. 4 *a* and *b* of Levin (1981); the results are summarized in column 2 of Table I of the present paper. At very high frequencies the membranes behave capacitively. Therefore, changes in g_{me} or g_{mi} will not affect the high ν behavior of ϕ (see Fig. 4 *b* in Levin [1981] and column 3 of Table I in this paper). The effects of extracellular resistance tend to depress the high frequency behavior of ϕ below the monotonically rising curve [$\tan^{-1}(2\pi\nu\tau_\phi)$] expected of a single uninvaginated cell. An increase in C_{mi} or a decrease in C_{me} will tend to send more current into the extracellular space. This will exaggerate the effects of extracellular resistance

TABLE I
EFFECTS OF MEMBRANE PARAMETER VARIATION ON R_{IN} AND ϕ

Change in membrane parameter	Effect on R_{IN}	Effect on ϕ	
		Low frequency	High frequency
$C_{me}\uparrow$	0	+	+
$C_{mi}\uparrow$	0	+	−
$C_{me}\downarrow$	0	−	−
$C_{mi}\downarrow$	0	−	+
$g_{me}\downarrow$	+	+	0
$g_{mi}\downarrow$	+	+	0
$g_{me}\uparrow$	−	−	0
$g_{mi}\uparrow$	−	−	0

The qualitative effects of membrane parameter variation on the input resistance and phase angle of the admittance of a tissue. Quantities that are raised, lowered, and unchanged are labeled +, −, and 0, respectively.

and cause a further depression of ϕ at high ν. On the other hand, a decrease in C_{mi} or an increase in C_{me} will lessen the current in the extracellular space. Therefore, the effects of the extracellular space will be diminished, and the phase angle will be pushed up at high frequency. These observations are illustrated in Fig. 4 *a* of Levin (1981) and listed in column 3 of Table I in this paper. Table I shows how R_{IN} and ϕ change when any membrane parameter is changed. It is evident that a change in C_{me} or C_{mi} leaves a unique "signature." This suggests that it is possible to derive formulas that give the intervention-induced changes in C_{me} and C_{mi} in terms of gross changes in R_{IN} and ϕ. Since the changes in R_{IN} and ϕ are unique on a relatively gross level, these formulas are expected to be insensitive to experimental errors in R_{IN} and ϕ. On the other hand, Table I shows that the "signature" of a decrease (increase) in g_{me} is identical to the "signature" of a decrease (increase) in g_{mi}. This means that a method of distinguishing a change in g_{me} from a like change in g_{mi} will require the measurement of fairly subtle changes in the frequency dependence of ϕ. Therefore, one expects that a formula for the intervention dependence of g_{me} alone (or g_{mi} alone) might be sensitive to experimental errors in R_{IN} and ϕ. On the other hand, the intervention dependence of the total membrane conductivity (the sum of g_{me} and g_{mi}, weighted by the areas of surface and invaginated membranes, respectively) should be accurately calculable from measurements of the intervention dependence of R_{IN} and ϕ.

II. FORMULAS FOR CHANGES IN MEMBRANE CAPACITY AND CONDUCTIVITY

In this section I prove the formulas that determine the intervention-induced changes in membrane parameters in terms of the measured changes in R_{IN} and ϕ. The results are illustrated in the case of a preparation that behaves as a "lumped" circuit.

The following assumptions are used in the proof:

1) The tissue has a smooth external surface with total area S_e. The extracellular space is bordered by invaginated membranes with total surface area S_i. The extracellular space may be of any size or shape and is connected to the bath by well-defined mouths. As pointed out in section IV of Levin (1981), the electrical definition of "surface" membrane includes any membrane area that is connected to the bath by a sufficiently small series resistance. Specifically, the time constant of charging of the membrane must be $<1/2\pi\nu_M$, where ν_M is the highest frequency at which the linear response is measured.

2) The medium in the extracellular space is purely resistive. Its specific resistivity can be spatially heterogeneous.

3) The unit surface (invaginated) membrane is characterized by a spatially uniform admittance Y_e (Y_i). Most of the results in this paper will apply to the case in which Y_e (Y_i) is the admittance of an RC circuit; however, the method can be generalized to more complex unit membrane circuits at the cost of a certain amount of mathematical complexity (D. N. Levin, unpublished). Since the electrical characteristic of the invaginated membrane is assumed to be spatially uniform, the method cannot tolerate a "droop" of the steady-state voltage in the extracellular space. Therefore, if the linear characteristics of the preparation are measured at a nonresting holding potential, the invaginated membrane conductivity must be blocked. Notice that the formula for total external surface membrane capacity in Levin (1981) was proved without assuming the spatial uniformity of the membrane characteristics;

therefore, the results in Levin (1981) are valid even in the presence of a steady-state voltage gradient in the extracellular space.

4) The intracellular voltage drop between the electrodes and the membranes is negligible or accurately calculable. The standard experimental and theoretical methods of satisfying this condition are reviewed in section III A of Levin (1981).

5) The preparation is stable to electrical perturbations. This means that small steps in voltage (current) lead to small steps in current (voltage) after transients have disappeared.

6) A series of interventions, characterized by a parameter β, induces changes in Y_e and Y_i without changing the geometric configuration or resistivity of the extracellular space. For example, β might be the bath concentration of a pharmacological agent that diffuses uniformly into the extracellular space. β could also be the holding potential at which the linear characteristics of the preparation are measured; in this case, the invaginated membrane conductivity must be blocked as mentioned in 3. If there is evidence (Poole-Wilson et al., 1979) that the intervention (e.g., a protracted change in holding potential or a change in contractile state) changes the resistivity or geometry of the extracellular space, the methods of this paper are not applicable.

Let $y_m(p)$ be the admittance of the tissue; p is the Laplace transform variable. The proof of the basic formulas is begun by noticing that y_m can be written as

$$y_m = S_e Y_e + S_i Y_i F. \tag{1}$$

F is the fraction of the invaginated membrane that is conducting effectively even in the presence of extracellular resistance. Intuitively, one expects F to be a function of Y_i, the admittance of the membrane that faces the extracellular space. It is not difficult to see that the functional form of F's dependence on Y_i will be determined by the geometry of the extracellular space and the spatial variation of R_e. This statement is illustrated by Eqs. B3 and B8 in Levin (1981), which give the explicit forms of F for the "disk" model of a skeletal muscle fiber and the "pie" model of a cardiac Purkinje fiber.

Because of assumptions 6 and 2 the geometry and impedance of the extracellular space do not depend on β and p. Therefore, the functional dependence of F on Y_i is unaffected by changes in β or p. It follows from Eq. 1 that the dependence of y_m on β and p is mediated by the dependence of Y_e and Y_i on these variables. This means that

$$\begin{aligned} \frac{\delta y_m}{\delta \beta} &= S_e \frac{\delta Y_e}{\delta \beta} + S_i \frac{d(Y_i F)}{dY_i} \frac{\delta Y_i}{\delta \beta} \\ \frac{\delta y_m}{\delta p} &= S_e \frac{\delta Y_e}{\delta p} + S_i \frac{d(Y_i F)}{dY_i} \frac{\delta Y_i}{\delta p}. \end{aligned} \tag{2}$$

These equations can be combined to eliminate the function F, which contains all model-dependent information about the geometry and resistivity of the extracellular space:

$$\frac{\delta y_m}{\delta p} \frac{\delta Y_i}{\delta \beta} - \frac{\delta y_m}{\delta \beta} \frac{\delta Y_i}{\delta p} = S_e \left[\frac{\delta Y_e}{\delta p} \frac{\delta Y_i}{\delta \beta} - \frac{\delta Y_e}{\delta \beta} \frac{\delta Y_i}{\delta p} \right]. \tag{3}$$

This is the fundamental relation that allows the determination of the intervention dependence of the membrane parameters (i.e., $\delta Y_e/\delta\beta$, $\delta Y_i/\delta\beta$) in terms of the observed dependence of the

preparation's impedance on the intervention and on frequency (i.e., $\delta y_m/\delta\beta$, $\delta y_m/\delta p$). In the rest of this section this formula is applied to the case in which the external and internal membranes are characterized by RC circuits.

If the surface and invaginated membranes behave as RC circuits, then

$$Y_{\substack{e\\i}} = g_{\substack{me\\i}} + C_{\substack{me\\i}} p\,, \tag{4}$$

where g_{me} (g_{mi}) and C_{me} (C_{mi}) are the specific conductivity and capacity of the surface (invaginated) membrane. g_{me}, g_{mi}, C_{me}, and C_{mi} are expected to depend on β, the parameter that characterizes the intervention state. Substituting Eq. 4 into Eq. 3 and rearranging terms gives:

$$S_e \frac{\delta g_{me}}{\delta\beta} + \left(\frac{\delta D}{\delta p}\right)\frac{1}{C_{mi}}\frac{\delta g_{mi}}{\delta\beta} + \left(p\frac{\delta D}{\delta p}\right)\frac{1}{C_{mi}}\frac{\delta C_{mi}}{\delta\beta} = \frac{\delta D}{\delta\beta}\,, \tag{5}$$

where

$$D = y_m - S_e C_{me} p. \tag{6}$$

This equation is true at every point in the complex p plane. In Levin (1981) it was shown that measurements of R_{IN} and ϕ determine the value of D at any point in the right half-p-plane. To see this, recall that Eq. A3 of Levin (1981) gives a "phase representation" of y_m in the right half-plane:

$$y_m = S_e C_{me} H \Gamma, \tag{7}$$

where

$$\Gamma(p) = \exp\left[\frac{2}{\pi}\int_0^\infty d\omega\, \frac{\omega(\phi_H - \phi)}{\omega^2 + p^2}\right].$$

Here, the convergence factor H can be chosen to be

$$H(p) = \frac{1}{\tau_H} + p,$$

where τ_H is any positive number. ϕ_H is the phase of H on the imaginary p-axis: $\phi_H = \tan^{-1}(\tau_H\omega)$. Eq. A5 of Levin (1981) implies that

$$S_e C_{me} = \frac{1}{R_{IN} H(0)\Gamma(0)}\,. \tag{8}$$

Eqs. 6, 7, and 8 can be combined to give

$$D = \frac{1}{R_{IN} H(0)\Gamma(0)}(H\Gamma - p)$$

$$\frac{\delta D}{\delta p} = \frac{1}{R_{IN} H(0)\Gamma(0)}\left(\Gamma\frac{\delta H}{\delta p} + H\Gamma\frac{\delta I}{\delta p} - 1\right), \tag{9}$$

where

$$\frac{\delta I}{\delta p} = \frac{-4p}{\pi} \int_0^\infty d\omega \frac{\omega(\phi_H - \phi)}{(\omega^2 + p^2)^2} .$$

Therefore, measurements of R_{IN} and ϕ determine the values of D and $\delta D/\delta p$ at all points in the right half-plane. Eq. 9 also shows that the value of $\delta D/\delta\beta$ at any p can be calculated by measuring how R_{IN} and ϕ vary as β changes.

Eq. 5 can be written down at three different values of p: p_1, p_2, p_3:

$$\begin{aligned}
S_e \frac{\delta g_{me}}{\delta\beta} + \left(\frac{\delta D_1}{\delta p}\right) \frac{1}{C_{mi}} \frac{\delta g_{mi}}{\delta\beta} + \left(p_1 \frac{\delta D_1}{\delta p}\right) \frac{1}{C_{mi}} \frac{\delta C_{mi}}{\delta\beta} &= \frac{\delta D_1}{\delta\beta} \\
S_e \frac{\delta g_{me}}{\delta\beta} + \left(\frac{\delta D_2}{\delta p}\right) \frac{1}{C_{mi}} \frac{\delta g_{mi}}{\delta\beta} + \left(p_2 \frac{\delta D_2}{\delta p}\right) \frac{1}{C_{mi}} \frac{\delta C_{mi}}{\delta\beta} &= \frac{\delta D_2}{\delta\beta} \\
S_e \frac{\delta g_{me}}{\delta\beta} + \left(\frac{\delta D_3}{\delta p}\right) \frac{1}{C_{mi}} \frac{\delta g_{mi}}{\delta\beta} + \left(p_3 \frac{\delta D_3}{\delta p}\right) \frac{1}{C_{mi}} \frac{\delta C_{mi}}{\delta\beta} &= \frac{\delta D_3}{\delta\beta} .
\end{aligned} \tag{10}$$

Here, $\delta D_{1,2,3}/\delta p$ and $\delta D_{1,2,3}/\delta\beta$ denote derivatives evaluated at $p = p_1, p_2, p_3$. We can regard $\delta D/\delta p$ and $\delta D/\delta\beta$ as "knowns," since they are determined by measurements of R_{IN} and ϕ in each intervention state. Therefore, Eqs. 10 comprise three equations with three unknowns: S_e $\delta g_{me}/\delta\beta$, $1/C_{mi}\, \delta g_{mi}/\delta\beta$, and $1/C_{mi}\, \delta C_{mi}/\delta\beta$. Cramer's rule gives the solution

$$\begin{aligned}
S_e \frac{\delta g_{me}}{\delta\beta} &= \frac{Q}{M} \\
\frac{1}{C_{mi}} \frac{\delta g_{mi}}{\delta\beta} &= \frac{T}{M} \\
\frac{1}{C_{mi}} \frac{\delta C_{mi}}{\delta\beta} &= \frac{E}{M} ,
\end{aligned} \tag{11}$$

where M, Q, T, and E are determinants of matrices whose elements are measurable:

$$M = \begin{vmatrix} 1 & \frac{\delta D_1}{\delta p} & p_1 \frac{\delta D_1}{\delta p} \\ 1 & \frac{\delta D_2}{\delta p} & p_2 \frac{\delta D_2}{\delta p} \\ 1 & \frac{\delta D_3}{\delta p} & p_3 \frac{\delta D_3}{\delta p} \end{vmatrix}$$

$$= \frac{\delta D_2}{\delta p} \frac{\delta D_3}{\delta p} (p_3 - p_2) - \frac{\delta D_1}{\delta p} \frac{\delta D_3}{\delta p} (p_3 - p_1) + \frac{\delta D_1}{\delta p} \frac{\delta D_2}{\delta p} (p_2 - p_1)$$

$$Q = \begin{vmatrix} \frac{\delta D_1}{\delta \beta} & \frac{\delta D_1}{\delta p} & p_1 \frac{\delta D_1}{\delta p} \\ \frac{\delta D_2}{\delta \beta} & \frac{\delta D_2}{\delta p} & p_2 \frac{\delta D_2}{\delta p} \\ \frac{\delta D_3}{\delta \beta} & \frac{\delta D_3}{\delta p} & p_3 \frac{\delta D_3}{\delta p} \end{vmatrix}$$

$$T = \begin{vmatrix} 1 & \frac{\delta D_1}{\delta \beta} & p_1 \frac{\delta D_1}{\delta p} \\ 1 & \frac{\delta D_2}{\delta \beta} & p_2 \frac{\delta D_2}{\delta p} \\ 1 & \frac{\delta D_3}{\delta \beta} & p_3 \frac{\delta D_3}{\delta p} \end{vmatrix}$$

$$E = \begin{vmatrix} 1 & \frac{\delta D_1}{\delta p} & \frac{\delta D_1}{\delta \beta} \\ 1 & \frac{\delta D_2}{\delta p} & \frac{\delta D_2}{\delta \beta} \\ 1 & \frac{\delta D_3}{\delta p} & \frac{\delta D_3}{\delta \beta} \end{vmatrix}. \tag{12}$$

Eqs. 11 can be integrated from $\beta = \beta_1$ to $\beta = \beta_2$:

$$S_e[g_{me}(\beta_2) - g_{me}(\beta_1)] = \int_{\beta_1}^{\beta_2} d\beta \frac{Q}{M} \tag{13 a}$$

$$\frac{C_{mi}(\beta_2)}{C_{mi}(\beta_1)} = \exp\left(\int_{\beta_1}^{\beta_2} d\beta \frac{E}{M}\right) \tag{13 b}$$

$$\frac{g_{mi}(\beta_2) - g_{mi}(\beta_1)}{C_{mi}(\beta_1)} = \int_{\beta_1}^{\beta_2} d\beta \frac{T}{M} \exp\left(\int_{\beta_1}^{\beta} d\beta \frac{E}{M}\right). \tag{13 c}$$

These results can be cast in a more symmetrical form by noting that Eq. 8 implies

$$S_e C_{me}(\beta_1) = \frac{1}{[R_{IN} H(0)\Gamma(0)]_{\beta-\beta_1}}. \tag{14}$$

Dividing Eqs. 8 and (13 *a*) by the above expression gives Eqs. 15 *a* and 15 *b*

$$\frac{C_{me}(\beta_2)}{C_{me}(\beta_1)} = \frac{[R_{IN} H(0)\Gamma(0)]_{\beta-\beta_1}}{[R_{IN} H(0)\Gamma(0)]_{\beta-\beta_2}} \tag{15 a}$$

$$\frac{g_{me}(\beta_2) - g_{me}(\beta_1)}{C_{me}(\beta_1)} = [R_{IN} H(0)\Gamma(0)]_{\beta-\beta_1} \int_{\beta_1}^{\beta_2} d\beta \frac{Q}{M} \tag{15 b}$$

$$\frac{C_{mi}(\beta_2)}{C_{mi}(\beta_1)} = \exp\left(\int_{\beta_1}^{\beta_2} d\beta \frac{E}{M}\right) \tag{15 c}$$

$$\frac{g_{mi}(\beta_2) - g_{mi}(\beta_1)}{C_{mi}(\beta_1)} = \int_{\beta_1}^{\beta_2} d\beta \frac{T}{M} \exp\left(\int_{\beta_1}^{\beta} d\beta \frac{E}{M}\right). \tag{15 d}$$

Here, Eqs. 15 *c* and 15 *d* are identical to Eqs. 13 *b* and 13 *c*. The right side of each equation is determined by the directly measurable quantities, R_{IN} and ϕ. Therefore, the intervention dependence of the membrane parameters can be deduced from the experimental measurements without modeling the extracellular space and without fitting the model's parameters to the data curves, etc.

In an idealized experiment, Eqs. 15 *a–d* could be used according to the following prescription:

1) Manipulate the preparation continuously from one intervention state ($\beta = \beta_1$) to another intervention state ($\beta = \beta_2$). R_{IN} and the frequency dependence of ϕ are measured at all intervening values of β.

2) Pick any set of real positive values for p_1, p_2, p_3.

3) Use Eq. 9 and the measurements of R_{IN} and ϕ to calculate $\delta D_{1,2,3}/\delta p$ and $\delta D_{1,2,3}/\delta\beta$ at each value of β between β_1 and β_2.

4) Use Eq. 12 to determine the values of M, Q, T, and E at each value of β.

5) Calculate the intervention-induced changes in C_{me}, C_{mi}, g_{me}, and g_{mi} by performing the integrations over β on the right side of Eq. 15.

6) If S_e has been measured, use Eq. 14 to calculate $C_{me}(\beta_1)$.

7) Repeat steps 1–5 using the same data for R_{IN} and ϕ but using different values of p_1, p_2, p_3. In an exact analytical calculation the calculated changes in the membrane parameters must be the same. If the calculated values of the membrane parameters depend on the p_1, p_2, p_3 values used to analyze actual data, then an error is present. For example, the membranes may not be characterized by RC circuits, as assumed in assumption 3. Experimental errors in the data for R_{IN} and ϕ or numerical errors in the computation of the frequency domain integrals could also cause the results of the calculation to depend on the values chosen for p_1, p_2, p_3. Therefore, analyzing the data with different sets of p values constitutes a useful check on the accuracy of the whole procedure.

It is instructive to show that a simple "lumped" circuit (Falk and Fatt, 1964; see Fig. 1 of Levin [1981]) satisfies Eq. 15. The admittance of the lumped model is given by Eq. 1 with

$$F = \frac{1}{1 + R_S Y_i}. \tag{16}$$

The resistance of the extracellular space is represented by R_S and is assumed to be independent of the intervention parameter, β. D can be calculated explicitly from Eqs. 6, 1, and 16:

$$D = S_e g_{me} + \frac{S_i}{R_S}\left(1 - \frac{1}{1 + R_S Y_i}\right). \tag{17}$$

It follows that

$$\frac{\delta D}{\delta p} = \frac{S_i C_{mi}}{(1 + R_S Y_i)^2}$$

$$\frac{\delta D}{\delta \beta} = S_e \frac{\delta g_{me}}{\delta \beta} + \frac{S_i}{(1 + R_S Y_i)^2}\left(\frac{\delta g_{mi}}{\delta \beta} + p \frac{\delta C_{mi}}{\delta \beta}\right). \tag{18}$$

These equations show that the "lumped" model satisfies:

$$\frac{\delta D}{\delta \beta} = S_e \frac{\delta g_{me}}{\delta \beta} + \left(\frac{\delta D}{\delta p}\right)\frac{1}{C_{mi}}\frac{\delta g_{mi}}{\delta \beta} + \left(p \frac{\delta D}{\delta p}\right)\frac{1}{C_{mi}}\frac{\delta C_{mi}}{\delta \beta},$$

which is identical to Eq. 5. The rest of the proof which leads to Eqs. 15 is the same as in the general case.

III. APPLICATIONS

In order to apply Eqs. 15 to an actual experiment we need to modify the idealized prescription in section II. First, technical considerations require that ϕ be measured only over a limited frequency range: $\nu_0 < \nu < \nu_M$. In order to do the frequency domain integrals it is necessary to smoothly extrapolate ϕ into lower and higher frequency regions. Techniques for doing this were illustrated in Section III of Levin (1981). The accuracy of an actual experiment is also limited by the fact that R_{IN} and ϕ will be measured only in a small number of discrete intervention states characterized by $\beta = \beta_1, \beta_2, \beta_3 \ldots$. At each value of β, D and $\delta D/\delta p$ can be caluclated with the aid of Eq. 9. The integrands in Eqs. 15 are determined by $\delta D/\delta \beta$ and $\delta D/\delta p$; at $\beta = 1/2\ (\beta_1 + \beta_2)$ these quantities can be approximated by

$$\frac{\delta D}{\delta \beta} \approx \frac{D(\beta_2) - D(\beta_1)}{\beta_2 - \beta_1}$$

$$\frac{\delta D}{\delta p} \approx \frac{1}{2}\left(\frac{\delta D}{\delta p}\bigg|_{\beta_2} + \frac{\delta D}{\delta p}\bigg|_{\beta_1}\right). \tag{19}$$

These expressions will be accurate if D and $\delta D/\delta p$ are nearly linear in β between β_1 and β_2. The integrands in Eqs. 15 are evaluated at $\beta = 1/2(\beta_1 + \beta_2)$ by substituting the above equations into Eq. 12. The integral from β_1 to β_2 is estimated by multiplying the result by $\beta_2 - \beta_1$. Then, Eqs. 15 show how the membrane parameters change when the preparation is moved from one intervention state (β_1) to another (β_2). In the following two subsections this procedure is illustrated by applying it to synthetic data for R_{IN} and ϕ.

A. *Measurement of Voltage-dependent Capacitance*

Schneider and Chandler (1973) discovered that frog skeletal muscle fibers have a voltage-dependent capacity, which they attribute to a charge movement process. A unit membrane process of this kind will have an intrinsic time constant that is independent of the time constant associated with restivity in the extracellular space. At room temperature this intrinsic time constant may be as large as 1 ms, corresponding to a characteristic frequency of 160 Hz. This means that the unit membrane will not be represented by a simple RC circuit

throughout the usual frequency range of impedance measurements (e.g., 1–5,000 Hz). Specifically, the voltage-dependent capacity must be in series with a resistance that represents the sluggishness of the underlying process. Therefore, Eqs. 15, which were derived for RC circuits, are not applicable to this tissue.

On the other hand, it is likely that there are other syncytial preparations in which the membrane molecules undergo more rapid charge movement processes (e.g., intrinsic time constants $\lesssim 1/30$ ms or intrinsic frequencies $\gtrsim 5{,}000$ Hz). The unit membranes of such preparations will be represented by simple RC circuits over the range 1–5,000 Hz. In this case, Eqs. 15 can be used to calculate the voltage dependence of C_{me} and C_{mi} from measurements of the voltage dependence of R_{IN} and ϕ. This technique will be illustrated by considering a model of a syncytial tissue (for simplicity, the "disk" model of a muscle fiber) in which the unit membrane is represented by a resistance in parallel with a voltage-dependent

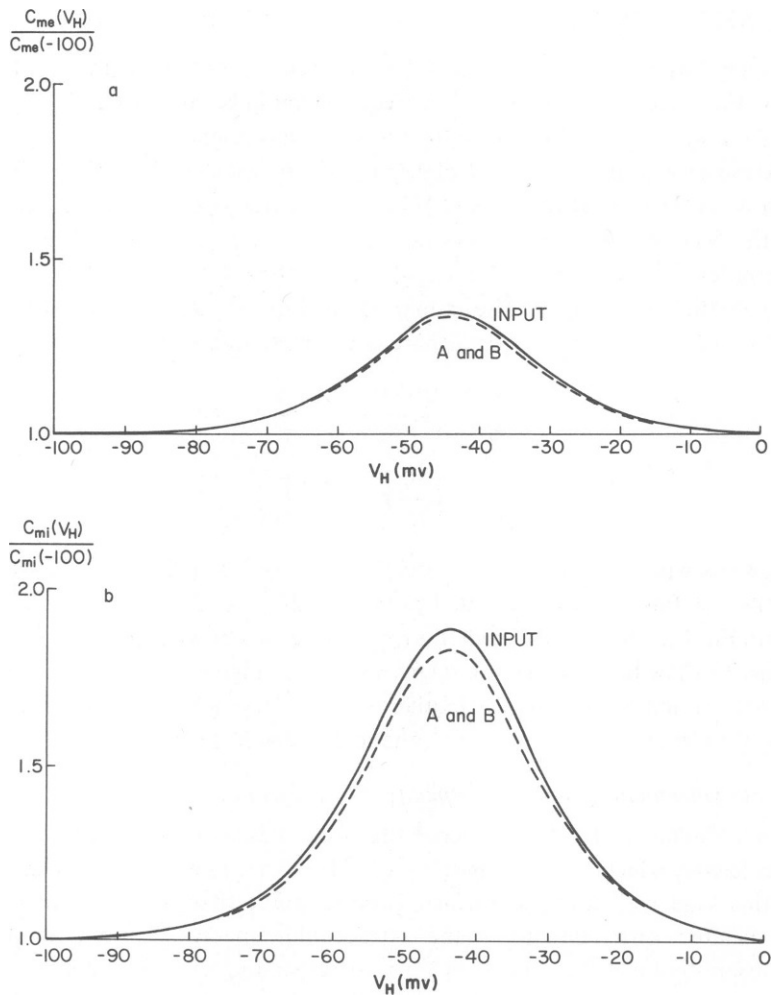

FIGURE 1. See legend on next page.

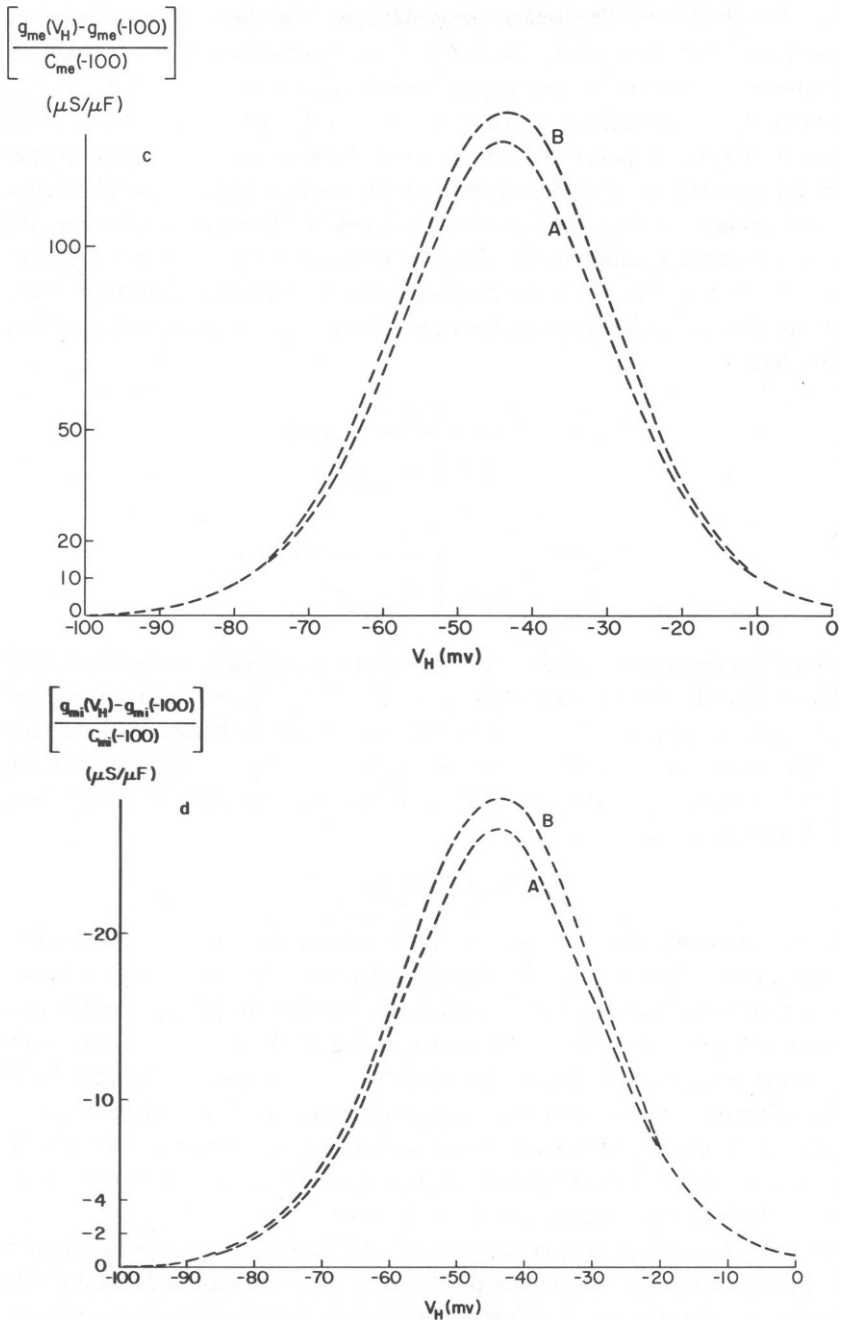

FIGURE 1 The solid ("input") lines in *a* and *b* show how the membrane capacities are assumed to depend on the holding potential V_H (see Eq. 20). These capacitances and small voltage-independent membrane conductances (see Eq. 21) are used in the skeletal muscle disk model to generate synthetic data for input resistance and phase angle (see Fig. 2). When these "data" are substituted in the right side of Eqs. 15, calculation shows that the underlying membrane capacities and conductivities must fall on the dashed lines in *a–d*. The labels *A* and *B* represent the results of the calculation when the "data" are analyzed with *A* or *B* values of the sliding parameters p_1, p_2, p_3.

capacitance. The model will be used to generate synthetic data for R_{IN} and ϕ at various holding potentials. Then, Eqs. 15 will be used to deduce the voltage dependence of membrane capacity from the "measured" voltage dependence of R_{IN} and ϕ.

The disk model of a skeletal muscle fiber has been described by Falk and Fatt (1964) and by Adrian et al. (1969); the pertinent features of the theory are also outlined in Appendix B of Levin (1981). I have taken the model's geometric parameters from the morphometric work of Mobley and Eisenberg (1975); these values are listed in Appendix B of Levin (1981). The specific resistivity of the medium in the T system is set equal to the resistivity of the Ringer's solution: $R_e \approx 100$ Ωcm. The electrical characteristics of the membranes were chosen in the following way. The membrane capacitances are taken to be functions of the holding voltage (V_H in millivolts):

$$C_{me} = 1 + \frac{0.35}{\cosh^2\left(\frac{V_H + 44}{16}\right)} \mu F/cm^2$$

$$C_{mi} = 1 + \frac{0.9}{\cosh^2\left(\frac{V_H + 44}{16}\right)} \mu F/cm^2. \tag{20}$$

The assumed dependence of C_{me} and C_{mi} on V_H is shown graphically by the solid lines in Fig. 1 *a* and *b*. Notice that the "extra" capacity (up to 0.35 $\mu F/cm^2$ for C_{me} and 0.9 $\mu F/cm^2$ for C_{mi}) reaches a maximum at $V_H = -44$ mV and then declines over a characteristic voltage interval of 8 mV. Membrane conductances must be blocked in any measurement of the voltage dependence of capacity. Therefore, g_{me} and g_{mi} are taken to be small and voltage independent (Adrian and Almers, 1974):

$$g_{me} = g_{mi} = 5\ \mu S/cm^2. \tag{21}$$

We could have assumed that g_{me} and g_{mi} were voltage dependent without affecting the calculation in any significant way. For simplicity, this was not done. Synthetic data for ϕ and R_{IN} are generated by substituting Eqs. 20 and 21 into the disk model of a skeletal muscle fiber. The resulting voltage dependence of ϕ is shown in Fig. 2. As V_H moves from -100 to -44 mV, the increase in C_{mi} is three times the increase in C_{me}. As discussed in section I and Table I, this is responsible for a rise in ϕ at low frequencies and a drop in ϕ at high frequencies, as shown in Fig. 2. These changes are reversed as V_H increases beyond -44 mV. The input resistance of the model is independent of V_H, since there is no change in membrane conductivity; a 1-mm length of fiber has $R_{IN} = 14.4$ MΩ.

The "data" for R_{IN} and ϕ are now substituted into Eqs. 15 to see whether these equations reproduce the known voltage dependence of C_{me} and C_{mi}. I have assumed that ϕ is "measured" only between $\nu_0 = 1$ Hz and $\nu_M = 5{,}000$ Hz. The frequency domain integrals are performed by smoothly extrapolating these data into higher and lower frequency regions, as discussed in Levin (1981). Furthermore, I have assumed that R_{IN} and ϕ are "measured" only at discrete values of the intervention parameter (V_H); namely, $V_H = -100, -90, -80, \ldots, -10, 0$ mV. Therefore, all derivatives and integrals with respect to β (i.e., V_H) must be approximated by discrete differences and sums. As discussed in section II, the "data" are processed with two

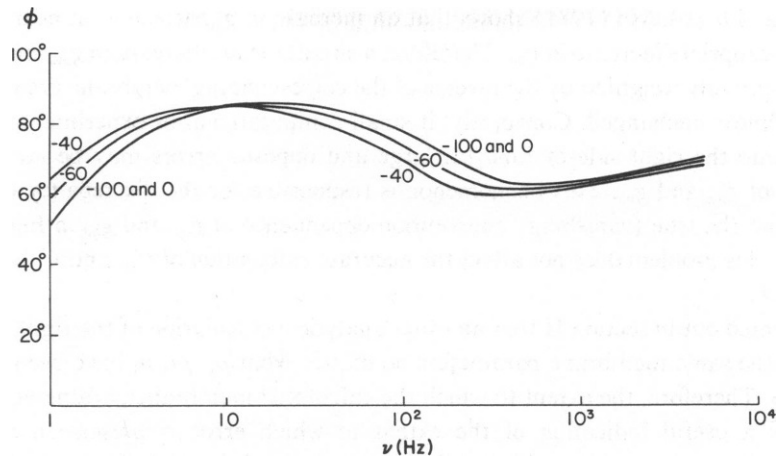

FIGURE 2 Synthetic data for the phase angle of the complex admittance (ϕ) of a 1-mm length of the skeletal muscle disk model. These "data" are generated by using small voltage-independent membrane conductances (Eq. 21) and voltage-dependent membrane capacitances (see Eq. 20 and the solid lines in Fig. 1 *a* and *b*). The curves are labeled by the voltage (V_H in mV) at which the fiber is held.

sets of values for p_1, p_2, and p_3:

$$(A)\ \frac{p_{1,2,3}}{2\pi} = 45, 500, 650 \text{ Hz}$$

$$(B)\ \frac{p_{1,2,3}}{2\pi} = 50, 250, 500 \text{ Hz}.$$

When the "data" and the A and B values of p are substituted into Eqs. 15, it is found that the membrane parameters must lie on the dashed lines, labeled A and B in Fig. 1 *a* and *b*.

The small discrepancy between the input and output values of C_{me} and C_{mi} can be attributed to several types of computational error:

1) The extrapolation of ϕ above 5,000 Hz and below 1 Hz was not exact, the extrapolated value differing by as much as 1.5° from the exact phase angle of the disk model.

2) Frequency domain integrals were performed on the computer as discrete sums with a typical sampling interval of 1 Hz.

3) Since R_{IN} and ϕ were "measured" only at discrete values of V_H, derivatives and integrals with respect to V_H were estimated by discrete differences and sums.

Even with these errors, the method produces good agreement between the computed and true voltage dependences of C_{me} and C_{mi}. This is because changes in C_{me} and C_{mi} leave a unique "signature" on the data (see Table I) that cannot be obliterated by small errors. The situation is quite different with regard to the calculation of membrane conductance from measurements of ϕ and R_{IN}. Fig. 1 *c* and *d* shows that the small errors of computation can produce relatively large discrepancies between the output (dashed lines) and input (zero) voltage dependence of g_{me} and g_{mi}. This can be understood in the following way. Table I shows that a change in g_{me} has the same qualitative effect on ϕ and R_{IN} as a change in g_{mi} in the same direction. For

example, Fig. 4 *b* in Levin (1981) shows that an increase in g_{me} affects ϕ in nearly the same way as an appropriate increase in g_{mi}. Therefore, a simultaneous increase in g_{me} and a decrease in g_{mi} (appropriately weighted by the inverse of the corresponding membrane areas) will leave R_{IN} and ϕ almost unchanged. Conversely, if small computational or experimental errors are introduced into the right side of Eqs. 15, large and opposite errors may be induced in the calculations of g_{me} and g_{mi}. This phenomenon is responsible for the discrepancy between the calculated and the true (vanishing) intervention dependence of g_{me} and g_{mi} in Fig. 1 *c* and *d*. Fortunately, this problem does not affect the accurate calculation of C_{me} and C_{mi}, as shown in Fig. 1 *a* and *b*.

It was pointed out in section II that an exact analytical calculation of the right side of Eqs. 15 will give the same membrane parameters no matter what p_1, p_2, p_3 have been used in the computation. Therefore, the extent to which the calculated membrane parameters depend on p_1, p_2, p_3 is a useful indication of the extent to which error is present in the data or computation. For example, suppose that the input values of C_{me} and C_{mi}, represented by the solid lines in Fig. 1 *a* and *b*, were not known. It would still be possible to conclude that the calculated C_{me} and C_{mi} (dashed lines) are accurate, since these calculated values are the same for the *A* and *B* values of p_1, p_2, p_3. On the other hand, the fact that the *A* and *B* values of *p* lead to different results for g_{me} (or g_{mi}) indicates that the conductivity calculations are significantly influenced by error.

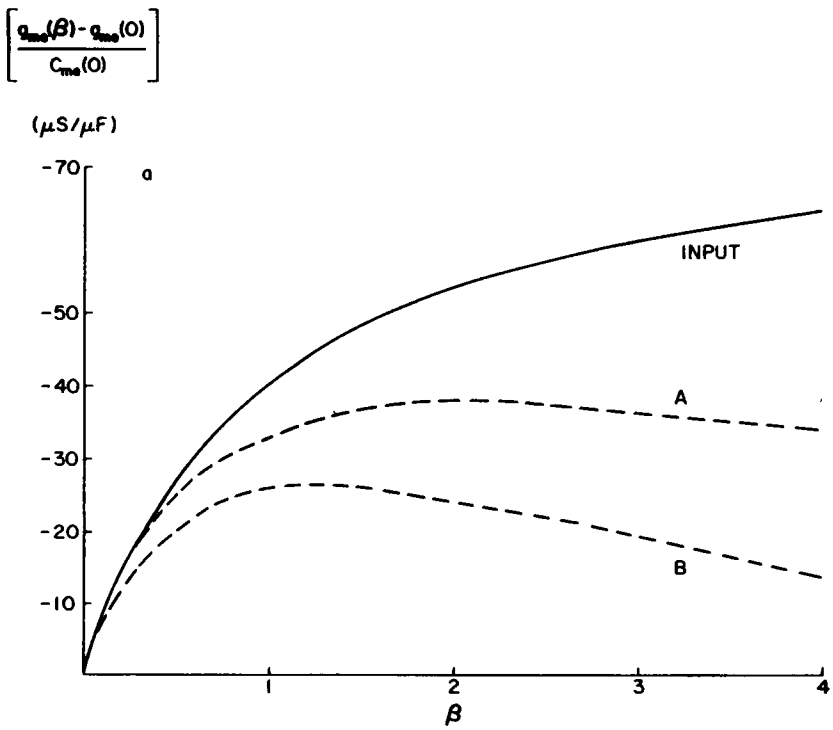

FIGURE 3

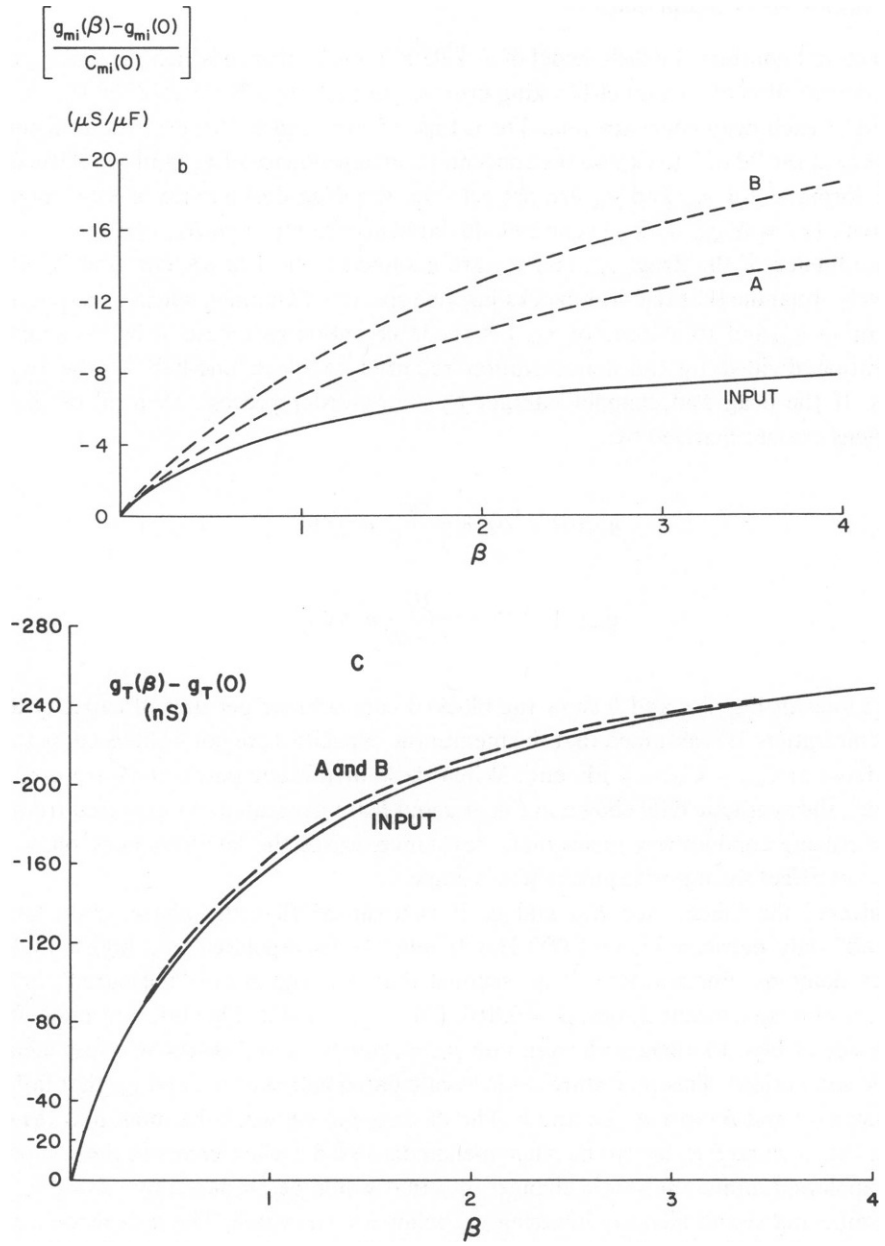

FIGURE 3 The solid ("input") lines show how the membrane conductivities are assumed to depend on β, the concentration of a channel-blocking drug in the bath (see Eq. 22). These conductances and fixed membrane capacitances (equal to 1 $\mu F/cm^2$) are used in the skeletal muscle disk model to generate synthetic data for phase angle and input resistance (Fig. 4 *a* and *b*). These "data" are then "inverted" with the aid of Eqs. 15. When the right side of Eqs. 15 is calculated with the A and B values for the sliding parameters p_1, p_2, p_3, the computed membrane conductivities fall on the dashed lines. Membrane capacities were calculated to change by <2% as β varies between 0 and 4.

B. *Measuring the Effects of Channel-blocking Agents on Membrane Conductance*

In this section I consider the disk model of a skeletal muscle fiber in which g_{me} and g_{mi} depend on the concentration of a channel-blocking drug in the bath. Synthetic data for R_{IN} and ϕ are generated at each drug concentration. Then, Eqs. 15 are used to "invert" the concentration dependence of the "data" to expose the concentration dependence of g_{me} and g_{mi}. Although the separate formulas for g_{me} and g_{mi} are not reliable, the drug dependence of total membrane conductivity ($g_T \equiv S_e g_{me} + S_i g_{mi}$) can be calculated accurately from R_{IN} and ϕ.

In the absence of the drug, g_{me} and g_{mi} are assumed to be 100 μS/cm^2 and 25 μS/cm^2, respectively. Imagine that the drug blocks just one species of channel, which is responsible for 80 μS/cm^2 of g_{me} and 10 μS/cm^2 of g_{mi}. Let the intervention parameter β be the actual drug concentration divided by the concentration required to block one-half of the blockable channels. If the drug and channel interact by a first-order process, then all of the above assumptions are summarized by:

$$g_{me}(\beta) = 20 + \frac{80}{1 + \beta}\ \mu\text{S/cm}^2$$

$$g_{mi}(\beta) = 15 + \frac{10}{1 + \beta}\ \mu\text{S/cm}^2. \tag{22}$$

The solid lines in Fig. 3 *a* and *b* show the blocked conductance per unit of capacity at each drug concentration. It is assumed that the membrane capacities are not influenced by the drug and are fixed at $C_{me} = C_{mi} = 1\ \mu$F/cm^2. When these membrane parameters are used in the disk model, the synthetic data shown in Fig. 4 *a* and *b* are generated. As expected from Table I, the decreasing conductivity raises input resistance, raises the low-frequency phase angle, and does not affect the high-frequency phase angle.

To "invert" the "data" for R_{IN} and ϕ, it is assumed that the phase angle has been "measured" only between 1 and 5,000 Hz. It must be extrapolated into higher and lower frequency domains. Furthermore, it is assumed that R_{IN} and ϕ are "measured" only at a discrete set of drug concentrations: $\beta = 0, 0.4, 0.8, \ldots, 3.6, 4.0$. This information is fed into the right side of Eqs. 15 along with values for p_1, p_2, p_3 (the *A* and *B* sets of values mentioned in the last subsection). This procedure leads to calculated values of g_{me} and g_{mi} that fall on the dashed lines (*A* and *B*) in Fig. 3 *a* and *b*. The discrepancy between the input and the output curves in Fig. 3 *a* and *b* is due to the phenomenon discussed earlier: errors in the computation and extrapolation mimic the subtle changes in ϕ that would be produced by raising g_{me} above its true value and simultaneously lowering g_{mi} below its true value. The p dependence of the calculated values of g_{me} and g_{mi} is another indication that they are in error. On the other hand, the calculated values of $C_{me}(\beta)/C_{me}(0)$ and $C_{mi}(\beta)/C_{mi}(0)$ are within 2% of unity, the input value.

Since the errors produced in calculating g_{me} and g_{mi} are in opposite directions, they should cancel out in the calculation of the drug dependence of total membrane conductivity ($g_T \equiv S_e g_{me} + S_i g_{mi}$). This quantity can be calculated accurately from R_{IN} and ϕ in the

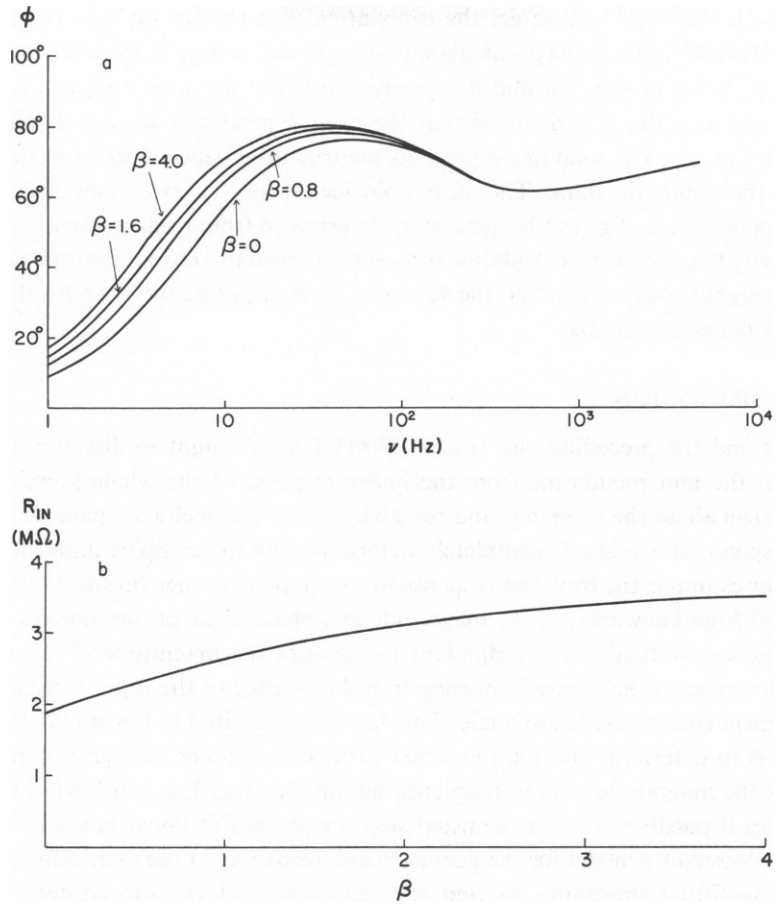

FIGURE 4 Synthetic data for the phase angle and input resistance of a 1-mm length of a skeletal muscle disk model which is exposed to a channel-blocking drug in concentration β. These "data" are generated by using fixed membrane capacitances (equal to 1 $\mu F/cm^2$) and drug-dependent conductivities (see Eq. 22 and the solid lines in Fig. 3 *a* and *b*).

following way:

$$g_T(\beta_2) - g_T(\beta_1) = S_e C_{me}(\beta_1)\left[\frac{g_{me}(\beta_2) - g_{me}(\beta_1)}{C_{me}(\beta_1)}\right] + S_i C_{mi}(\beta_1)\left[\frac{g_{mi}(\beta_2) - g_{mi}(\beta_1)}{C_{mi}(\beta_1)}\right]. \quad (23)$$

Eqs. 15 *b* and 15 *d* can be used to calculate the two quantities in brackets on the right from R_{IN} and ϕ. Similarly, Eq. 14 gives the factor $S_e C_{me}(\beta_1)$ in terms of R_{IN} and ϕ. The remaining factor on the right, $S_i C_{mi}(\beta_1)$, can be measured if β_1 corresponds to an intervention state in which all channels are blocked; then, $S_i C_{mi}(\beta_1)$ is just the total capacity in the β_1 state minus $S_e C_{me}(\beta_1)$ (given by Eq. 14). Of course, in a realistic experiment a small number of channels will not be blocked in the β_1 state. Therefore, there will be a small error in the measurement of total capacity in the β_1 state (e.g., errors <5% in the capacity measurements of Adrian and

Almers [1974]); this error will affect the calculation of $g_T(\beta_2)$ in Eq. 23. To illustrate the reliability of this technique we have calculated the right side of Eq. 23 from the synthetic data for R_{IN} and ϕ shown in Fig. 4 *a* and *b*; it is assumed that the total capacity is accurately measured in the β_1 state. It is deduced that the drug dependence of g_T is described by the dashed line in Fig. 3 *c*. The solid line represents the true drug dependence of g_T that was used to generate the synthetic data. The near coincidence of the two lines shows that the intervention dependence of g_T can be accurately determined from measurements of R_{IN} and ϕ. The insensitivity to error in the calculation of g_T is confirmed by the fact that the calculated g_T values do not significantly depend on the values of p_1, p_2, p_3 (e.g., the A or B values) used in the frequency domain integrals.

IV. DISCUSSION

In this paper and the preceding one (Levin, 1981) I have sought to discover what can be learned about the unit membrane from the linear response of the whole preparation when nothing is known about the geometry and resistivity of the extracellular space. It is clear that the linear response of a tissue is completely determined by the complex admittance at each frequency. For example, the transient response to a step (or any other variation) in voltage can be constructed from knowledge of the magnitude and phase angle of the complex admittance at each frequency. Actually, it is redundant to measure the magnitude of the admittance, since it can be constructed at any frequency from knowledge of the input resistance and the frequency dependence of the phase angle. This fact was exploited in Levin (1981) in order to use R_{IN} and ϕ to determine the total external surface membrane capacity, a quantity that characterizes the magnitude of high-frequency admittance (see Eq. 1 in Levin [1981]). This formula makes it possible to avoid the usual steps in analysis of linear behavior of syncytial tissues: (*a*) proposal of a model for the geometry and resistivity of the extracellular space; (*b*) use of a curve-fitting procedure to find the parameters of the extracellular space and membrane that are consistent with the phase angle data. The formula for total surface capacity is particularly useful for measuring how an arbitrary intervention affects the surface area or specific capacitance of the surface membrane.

In the present paper I have considered a restricted class of interventions, i.e., those that affect the membrane characteristics without influencing the geometry or resistivity of the extracellular space. If the membrane is assumed to behave as an RC circuit, the intervention-induced changes in membrane capacitance and conductance can be expressed directly in terms of measured changes in R_{IN} and ϕ (see Eqs. 15). Once again, it has been possible to sidestep the curve-fitting that is associated with models of the extracellular space and models of the intervention dependence of the membrane parameters. These methods may be useful in several types of experiment. For example, if membrane conductivity is blocked and transmembrane voltage is varied with electrodes, Eqs. 15 can be used to measure the voltage dependence of charge movements with short time constants (e.g., those $<1/30$ ms). As demonstrated in section III A, this method allows the determination of the relative amounts of charge movement on the surface and invaginated membranes. To analyze slower charge movements (e.g., those in frog skeletal muscle; see Schneider and Chandler [1973]) it is necessary to consider unit membranes that are not RC circuits. In that case, Eq. 3 gives a set of first-order,

coupled, *nonlinear* differential equations for the intervention-dependence of the membrane parameters in terms of R_{IN} and ϕ. Because of their nonlinearity, solutions of these equations cannot be written down in a closed form analogous to Eq. 15. The differential equations must be solved on a computer. It remains to be seen whether this can be done in a practical way.

As illustrated in section III B, Eqs. 23, 15, and 14 make it possible to measure how total membrane conductance is changed by the addition of channel-blocking agents or by variation of the bath concentration of the permeant ions. In this way one could determine the relative contributions of different channels to total conductivity without large errors due to resistance in the extracellular space. It may also be possible to measure how total membrane conductance changes as the resting potential is manipulated by variation of the bath potassium concentration.

In any application it is necessary to pay close attention to the role of the experimental error present in the data for R_{IN} and ϕ. Estimated errors in R_{IN} and ϕ must be followed as they propagate through the calculation of the right side of Eqs. 15. The output of the calculation will be a confidence band within which the membrane parameters are supposed to lie. For example, each output line (dashed) in Fig. 1 will be replaced by a blurred band when real data (rather than synthetic data) are used. In an exact analytical calculation, Eqs. 15 will give the same result for all choices of p_1, p_2, p_3. Therefore, in a realistic calculation the confidence bands for the membrane parameters must overlap for all choices of p_1, p_2, p_3. This is a good check on the reliability of the calculation. The propagation of experimental error and the width of the confidence band will be influenced by the p values used in the calculation. Therefore, the calculation should be made with many different choices of p_1, p_2, p_3. The membrane parameters can be considered to lie in the narrowest confidence band generated in this way.

The author would like to acknowledge many helpful and stimulating discussions with H. A. Fozzard and R. S. Eisenberg.

This research was supported in part by U. S. Public Health Service Program Project HL-20592.

Received for publication 8 April 1980 and in revised form 11 February 1981.

REFERENCES

Adrian, R. H., and W. Almers. 1974. Membrane capacity measurements of frog skeletal muscle in media of low ion content. *J. Physiol. (Lond.)*. 237:573–604.

Adrian, R. H., W. K. Chandler and A. L. Hodgkin. 1969. The kinetics of mechanical activation in frog muscle. *J. Physiol. (Lond.)*. 204:207–230.

Chandler, W. K., M. F. Schneider, R. F. Rakowski, and R. H. Adrian. 1975. Charge movements in skeletal muscle. *Phil. Trans. R. Soc. Lond. B Biol. Sci.* 270:501–505.

Falk, G., and P. Fatt. 1964. Linear electrical properties of striated muscle fibers observed with intracellular electrodes. *Proc. R. Soc. Lond. B Biol. Sci.* 160:69–123.

Levin, D. N. 1981. Surface capacity of electrically syncytical tissue. *Biophys. J.* 35:127–146.

Mobley, B. A., and B. Eisenberg. 1975. Sizes of components in frog skeletal muscle measured by methods of stereology. *J. Gen. Physiol.* 66:31–45.

Poole-Wilson, P. A., P. D. Bourdillon, and D. P. Harding. 1979. Influence of contractile state on the size of the extracellular space in isolated ventricular myocardium. *Bas. Res. Cardiol.* 74:604.

Schneider, M. F., and W. K. Chandler. 1973. Voltage dependent charge movement in skeletal muscle: a possible step in excitation-contraction coupling. *Nature (Lond.)*. 242:244–246.